

J. F. Agassant¹, F. Baaijens³, H. Bastian⁴, A. Bernnat⁴, A. C. B. Bogaerds³, T. Coupez¹, B. Debbaut⁸, A. L. Gavrus¹, A. Goublomme⁸, M. van Gurp⁵, R. J. Koopmans⁷, H. M. Laun⁶, K. Lee², O. H. Nouatin¹, M. R. Mackley^{2*}, G. W. M. Peters³, G. Rekers⁵, W. M. H. Verbeeten³, B. Vergnes¹, M. H. Wagner⁴, E. Wassner⁶ and W. F. Zoetelief⁵

¹CEMEF, Ecole des Mines de Paris, Sophia Antipolis, France

²Department of Chemical Engineering, University of Cambridge, Cambridge, UK

³Technical University of Eindhoven, Eindhoven, The Netherlands

⁴IKT, University of Stuttgart, Stuttgart, Germany

⁵DSM Research, Geleen, The Netherlands

⁶BASF, Ludwigshafen, Germany

⁷Dow Benelux, Terneuzen, The Netherlands

⁸Polyflow, Louvain-la-Neuve, Belgium

The Matching of Experimental Polymer Processing Flows to Viscoelastic Numerical Simulation

This paper describes work carried out in order to match experimental processing flows to numerical simulation. The work has brought together a consortium that has developed reliable experimental methods by which processing flows can be achieved in the laboratory and then ranked against numerical simulation.

A full rheological characterisation of a selected range of polymers was made and the results compared from different laboratories. The data was fitted to a number of rheological models. Multi-mode parameter fitting was universal for the linear viscoelastic response. Particular attention was paid to the non linear response of the material. Prototype industrial flow experiments were carried out for a number of geometries in different laboratories and the flow birefringence technique was used to map out the experimentally observed stress fields for different polymers in a range of complex flows that contained both extensional and shear flow components. Numerical simulation was carried out using a number of algorithms and a range of constitutive equations.

In order to make a quantitative comparison between experiment and simulation, an Advanced Rheological Tool (ART) module was developed that was able in some cases to quantify the level of fit between the numerically predicted and the experimentally observed stress patterns. In addition the ART module was able to optimise certain non-linear parameters in order to improve the quality of fit between experiment and simulation.

* Mail address: M. Mackley, Dept. Chem. Eng., University of Cambridge, Pembroke St., Cambridge CB2 3RA, UK

1 Background

Polymer processing is now a highly sophisticated and important commercial process, where typical annual world manufacture for bulk polymers such as polyethylene is of order 160 million tonnes. It is therefore increasingly important that both resin manufacturers and polymer converters have the ability to simulate, and thereby understand, the complexities of polymer manufacture in order that processes can be properly designed and optimised.

Coupled with the growth in size and scale for polymer fabrication, the last two decades, in particular, have seen significant advances in the science of polymer processing. With the advent of reliable and sophisticated rheometers, rheological characterisation has become more advanced and with this, advances in rheological constitutive equations have also occurred, see for example [1, 2, 3, 4]. In addition, this period has also seen the spectacular development of numerical techniques that now make it possible to solve complex constitutive equations for complex flow geometries [5, 6, 7, 8, 9, 10, 11, 12]. It is now possible to model genuine engineering flows using complex viscoelastic simulation and it is this aspect that is of direct concern to this project and paper. In this paper we report on the progress that has been made to match the simulation of "prototype industrial flows" with their laboratory counterparts. In addition we develop a way in which the quality of fit can be quantitatively assessed and also develop a method for the optimisation of certain constitutive parameters.

The work clearly builds on a large scientific literature relating to the characterisation and modelling of viscoelastic flows. The idea of matching simulation with experiment is relatively new. Early work by [13, 14, 15, 16], all represent landmarks in the evolution of applying advanced numerical modelling to

genuine processing situations. In all cases the method of rheological characterisation, the choice of constitutive equation and the choice of numerical techniques were all crucial aspects.

A team was formed to tackle this problem and the authorship of this paper gives an outline of the teams and also the main people involved in each of the centres. In this paper the evolution of work will be described in the following sections. In section 2, the important issue of characterisation and constitutive equations was considered. This raised many interesting experimental and modelling issues, some of which will be briefly considered in the section. In section 3, the development of a number of laboratory “prototype industrial flows” will be described and the diversity of different apparatus enabled a broad range of processing flow situations to be explored. In section 4, the numerical techniques used by different team members will be introduced. Section 5, contains the development of the “Advanced Rheological Tool” (ART) which is the numerical tool that is able to rank numerical simulation against experimental observation and also optimise certain rheological parameters. Finally in section 6 we review our findings and give future perspectives for the subject.

2 Rheological Characterisation and Choice of Constitutive Equation

The choice of an appropriate constitutive equation and the way the rheological parameters of the constitutive equation are derived from experimental data is central to the ability to successfully model a viscoelastic flow process. The classic way that this has been used in the past is to choose a particular constitutive equation and then fit the model to certain rheometric data. A well known early example of this approach is the work by Wagner and Laun [17], where they fitted linear viscoelastic oscillatory data to a multi mode Maxwell model and then matched non linear step strain data to an Integral Wagner constitutive equation. Others, such as [18, 19]; have fitted data to the differential multimode PTT, Phan Thien Tanner [20] or Giesekus [21] models and more recently models such as the Pom Pom [3, 22, 23, 24] and Molecular Stress Function [25, 26], have been used. In each case the model fitting parameters are established from rheometric, rheological experimental measurements that are separate from any particular commercial flow process.

As an example of classic rheological data, two sets of data are shown in Figs. 1 and 2. In Fig. 1, linear viscoelastic data (LVE) is presented. The link between the relaxation strength g_i of a Maxwell model and the storage and loss modulus G' and G'' is given by the equations.

$$G' = \sum \frac{g_i \lambda_i^2 \omega^2}{(1 + \lambda_i^2 \omega^2)}, \quad G'' = \sum \frac{g_i \lambda_i \omega}{(1 + \lambda_i^2 \omega^2)},$$

where λ_i is the relaxation time for each elastic element g_i . The fitting of the data to this model presents certain difficulties because it is a well known, “ill posed problem” with no unique solution [27, 28]. A choice has to be made whether to use a continuous or discrete spectrum and up to now, a discrete spectrum has been generally chosen. A choice then has to be made in terms of how many relaxation modes are chosen and how

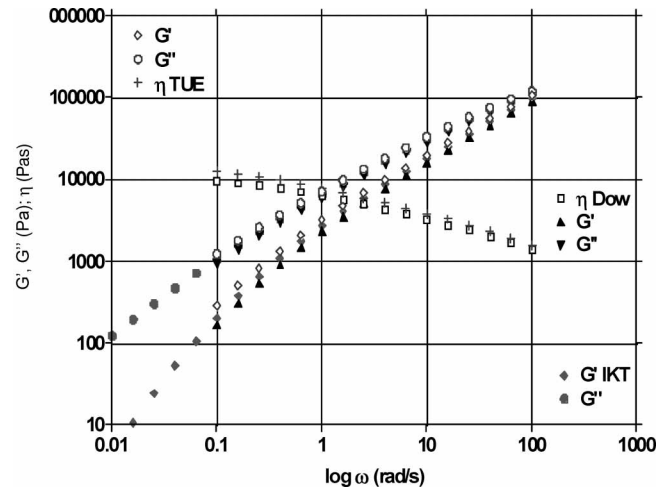


Fig. 1. Comparison of linear viscoelastic data for polyethylene at 190°C, obtained from three laboratories: IKT, Stuttgart, Germany; Eindhoven Technical University and Dow, Terneuzen, The Netherlands

the fitting of the model parameters is carried out. There are a number of different approaches but a pragmatic route is to choose say between 5 to 10 modes and use a least squares fitting routine. Many oscillatory rheometers have associated software packages that will perform these calculations automatically. Fig. 1 is an example of the type of data used to fit the linear viscoelastic relaxation modes. In general a good fit can be obtained, but it must be remembered that the parameters derived for the relaxation spectrum are not unique. Within the ART project we found that there was good agreement to within say 5 %, for LVE data obtained from different laboratories and from different rheometers. Fig. 1 shows different sets of data obtained from different laboratories. The greatest limitation appears to be the frequency range that can be explored by any one machine, however to some extent the use of time temperature superposition can overcome this difficulty. In general we are of the opinion that LVE data obtained from small strain oscillatory experiments is reliable and not subject to severe uncertainty.

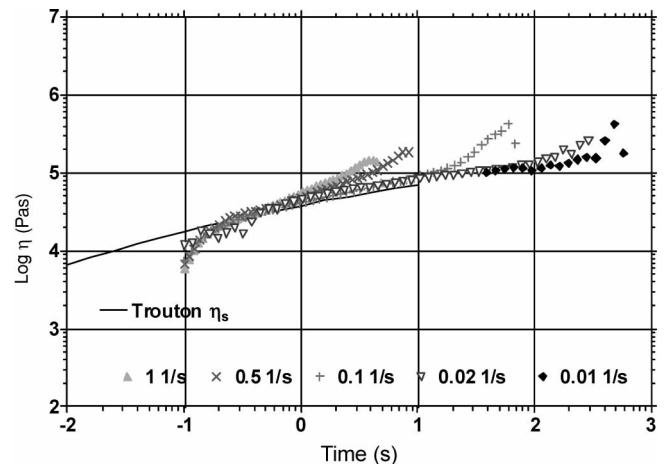


Fig. 2. Extensional uniaxial viscosity data obtained for polyethylene at 190°C. This was the type of rheometric data used to fit non linear model parameters, see for example [12]

The fitting of non linear parameters from rheometric data is a very much more challenging problem and there are still open issues in relation to the most appropriate experimental data and constitutive equation to use. Fig. 2 shows the fitting of some uniaxial extensional data to a rheological model and it is this general area that we have experienced greatest diversity for both the measurement and modelling of polymer melt flow.

An objective of the ART module was to overcome some of these difficulties by fitting the non linear rheology to flow birefringence data obtained from mixed (both shear and elongational) flows. Clearly the parameters obtained by the ART approach will need to give self consistency with the rheometric non linear experiments. However we believe that the use of more general deformations to obtain non linear parameters may result in greater final accuracy for the prediction of processing flows.

Progress has been made in the constitutive modelling of the rheology of polymer melts. The Technical University of Eindhoven, The Netherlands, have concentrated on the improvement of differential models [24], while the IKT, University of Stuttgart, Germany, have advanced the predictive capabilities of integral models [25].

3 Prototype Industrial Flows (PIF)

In order to fit a chosen rheological constitutive equation to a general processing flow it was necessary to develop a series of experimental prototype industrial flows, where laboratory scale experiments could be carried out and flow birefringence and other data obtained. This article reviews four geometries that were used and discusses the reasons behind their particular choice. The geometric configuration of each geometry is schematically shown in Fig. 3.

3.1 The Smooth Convergent Die (SCD)

The CEMEF laboratory at Sophia Antipolis, Ecole des Mines de Paris, France, have been working on a “two dimensional” slit die configuration that includes a smooth entry convergent flow [29, 30]. This flow geometry is shown schematically in Fig. 3 and a flow birefringence example is given in Fig. 4. The smooth convergent die (SCD) flow contains a shaded area shown in Fig. 3 where the flow is essentially extensional. The smooth convergence avoids experimental and numerical difficulties associated with sharp edges and in addition extends the region of the extensional flow. High quality images of the flow birefringence for different polyethylenes have been obtained for different screw extruder mass flowrates

3.2 The Cross Slot Apparatus (CSA)

Eindhoven Technical University, The Netherlands, have pioneered the use of the Cross Slot Apparatus (CSA) for the quantitative measurement of flow birefringence for polyethylene in pure extensional flow [31, 32, 11]. A schematic diagram of the geometry is shown in Fig. 3 and a diagram of the observed birefringence and matching simulation for an extended Pom

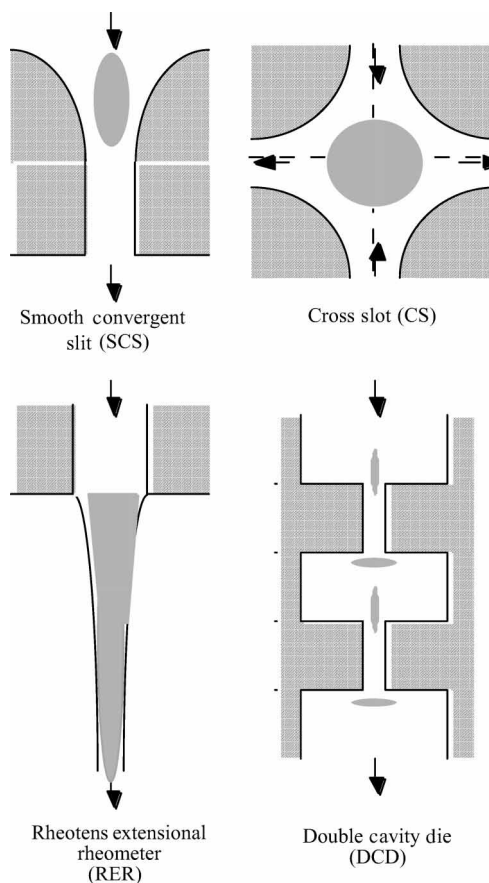


Fig. 3. Schematic of four prototype industrial flow (PIF) geometries showing shaded extensional flow regions for each geometry

Pom model is shown for a sector of the flow in Fig. 5. The flow at, and near the central stagnation point of the flow is pure elongation and because there is a stagnation point at the centre of the flow geometry, the level of strain subjected to material elements increases inversely with distance from the exit symmetry plane. This means that with this geometry it is possible to explore very high strains in an extensional deformation.

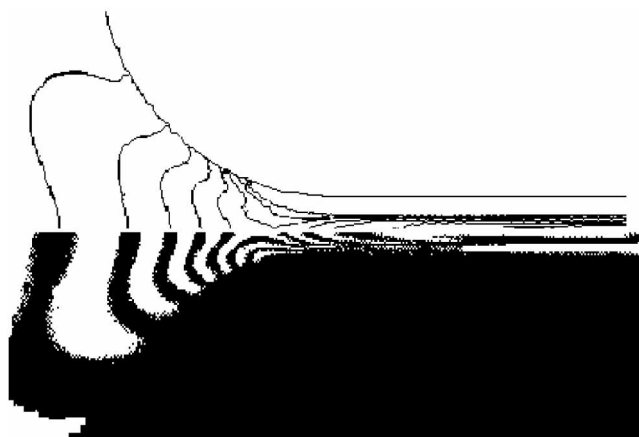


Fig. 4. Experimental and matching numerical simulation data for the smooth convergent die geometry (CEMEF, Ecole des Mines de Paris, Sophia-Antipolis, France) of HDPE, Stamylen HD8621, $T = 190^{\circ}\text{C}$, see [29] for further details

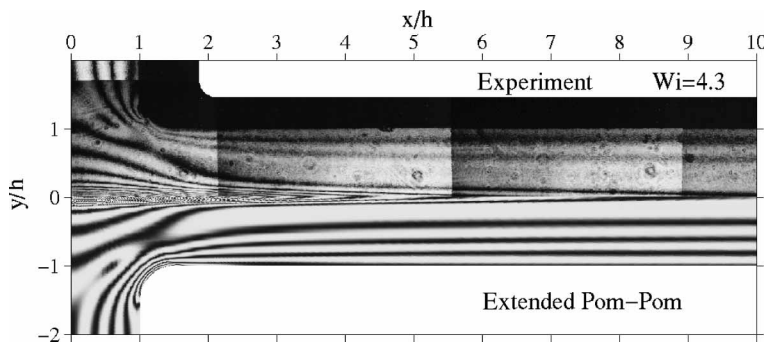


Fig. 5. Measured (top) and calculated (bottom) isochromatic fringe patterns for the extended Pom-Pom model at $We = 4.3$ of LDPE, DSM Stamylan LD 2008 XC43, $T = 150\text{ }^\circ\text{C}$, $lcn = 3.4294\text{ [s]}$, $u2D = 3.1\text{ [mm/s]}$, see [12, 24] for further details

3.3 Rheotens Extensional Rheometer (RER)

IKT, University of Stuttgart, Germany, have investigated the rheology of the Rheotens extensional rheometer which is shown schematically in Fig. 3 with data output shown in Fig. 6 [33, 34, 35]. The Rheotens involves a processing extrusion flow followed by a very controlled fibre draw down (FDA) of the molten polymer filament. For this experiment, it is not possible to follow the stress distribution by flow birefringence techniques. In this case, as shown in Fig. 6, the drawn down tensile force is therefore measured as a function of the different differential draw down velocities between the die exit and the draw down wheel. The apparatus is capable of generating very high elongational rates and is of course very similar to a classic commercial fibre-spinning operation.

3.4 The Double Cavity Die (DCD)

Cambridge University have been developing a double piston Multipass rheometer [36, 37] and they have used this for flow

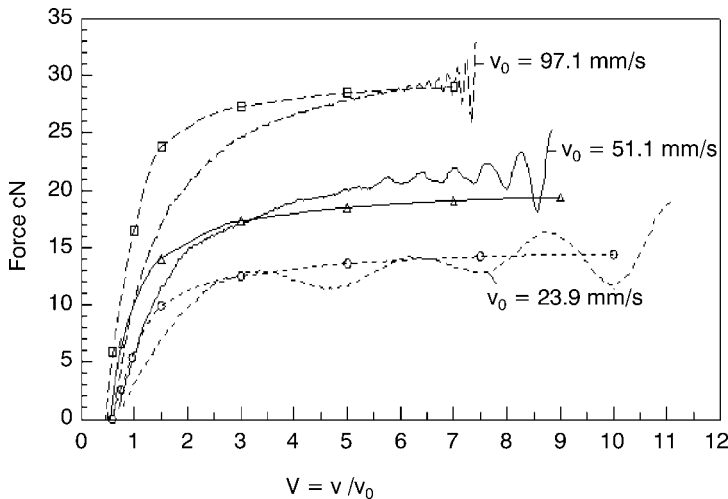


Fig. 6. Comparison of experimental (lines) and simulation (lines with symbols) for Rheotens curves of HDPE, DSM Stamylan, HD8621 for various flow rates, die $L/D = 15$ ($50\text{ }^\circ\text{C}$), see [35] for further details

birefringence studies of small quantities of polymer. They have chosen to follow the time dependant flow birefringence of polyethylene flowing backwards and forwards through a Double Cavity Die (DCD) of the type shown schematically in Fig. 3 and in reality by Fig. 7. Two servo hydraulically driven pistons force molten polymer in both directions through two cavities and the difference in the observed stress fields between the first and second cavity has been found to be particularly sensitive to the molecular architecture of the polyethylene under study [38].

4 Numerical Simulation

Modelling viscoelastic flow in complex geometries, such as the (PIF) geometries remains a challenging problem and in particular handling convergence difficulties at high Weissenberg numbers and stress singularities at sharp corners, have been two major difficulties in the past. Accurate finite element methods have now however been developed which allow the solution of generic constitutive equations such as (Oldroyd B – Phan Thien Tanner; and others) in 2D geometries. Finite element numerical codes (FENC) are now used successfully for more realistic constitutive equations that capture many of the characteristics of polymer processing flow. In this paper we describe three FENC which have been used in the ART program: Polyflow is a commercialised program from the Fluent group. Venus is a code that has been developed at Eindhoven University, and Seve 2 a code developed at CEMEF/Ecole des Mines de Paris. Some of these FENC are currently being extended to 3D viscoelastic flow computations, but this aspect will not be discussed in this paper.

Details relating to each code can be found in the following references. Polyflow [39, 40]. Venus [41], Seve 2 [18]. In this paper we just describe some of the main features of each code and their differences.

4.1 Form of Constitutive Equations

Polyflow is able to use both integral and differential equations in 2D geometries [13, 42]; and differential constitutive equations in both 2D and 3D geometries [43, 44], whilst Venus [41] and Seve 2 [18] use differential constitutive equations. The differential codes are able to march in time, however the integral code is at present a steady state solver.

4.2 The Formulation of the Equations

Polyflow and Seve 2 solve directly the equations for the mass balance, the force balance and the constitutive equations as a three-field problem, (velocity, pressure and extra stress components). In particular, for differential models, the 4×4 sub element interpolation with streamline upwinding technique [7] as well as the EVSS technique [6] are implemented in Polyflow, the latter technique is available for both 2D and 3D flow simula-

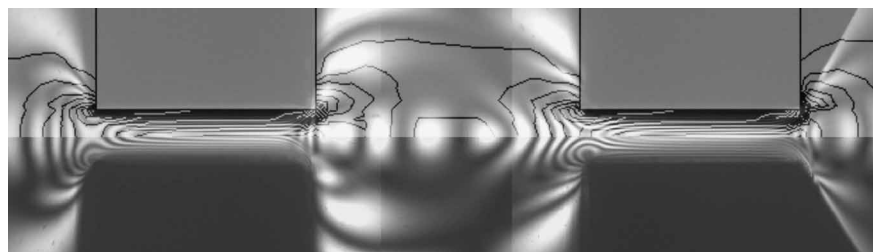


Fig. 7. Comparison of the overall experimental flow-birefringence pattern for a MPR experimental birefringence pattern with the simulated PSD for LLDPE, Dow, MI = 1, with flow conditions in a double cavity die of 1.84 g/min (apparent wall shear rate in the slit ~ 44 1/s) and 190 °C. The fringe pattern at cavity 1 (mushroom shape) and cavity 2 (butterfly shape) was captured by the Wagner model simulations. The increment of PSD contour lines is $2.95 \cdot 10^4$ Pa (C, $1.74 \cdot 10^{-9}$ 1/Pa), see [38] for further details

tions. Venus uses a DEVSS formulation (Discrete Elastic-Viscous Split Stress) which consists of adding the rate of strain tensor as an unknown and then solving a four-field problem (velocity, pressure, extra stress and rate of stress) [12].

4.3 The Finite Element Discretisation

Polyflow and Venus use quadrangle and triangles meshes and Seve 2 uses triangular meshes. In each case the compatibility conditions between the approximation spaces (for velocity, pressure and the different extra stress components) are assured. For example Seve 2 uses a quadratic approximation for the velocity, a linear discontinuous approximation for the pressure and a quadratic discontinuous approximation for the extra stress components. Similar features for the velocity and pressure are available in Polyflow. However, the interpolation for the viscoelastic extra-stress tensor depends on the selected algorithm: a linear continuous interpolation for the elastic part if the EVSS algorithm is used, and a quadratic or 4×4 subelement interpolation otherwise.

4.4 Numerical Solution Techniques

In general, the classical Galerkin method fails for viscoelastic flows because of the convective term ($u \cdot \nabla T u$) in the constitutive equation and because of stress singularities. This leads to a divergent numerical scheme even at low elasticity. Different upwinding techniques have been introduced to account for the hyperbolic character of the constitutive equations: Stream line Upwind (SU) or Stream line upwind Petrov Galerkin (SUPG) methods for Polyflow, Discontinuous Galerkin method for Venus and Seve 2.

4.5 The Numerical Solver

After discretisation, one obtains a set of non linear constitutive equations which are solved either by a Newton method for differential models or a decoupled method for integral models (Polyflow), a quasi Newton method, (Seve 2), or a GMRES method (Venus). Numerical solutions can be obtained from each solver and in this paper the output is presented as contours of principal stress difference for the different prototype industrial flows being considered (see Figs. 4, 5 and 9).

5 The ART Module

We have established the performance of numerical simulation by comparing the numerically predicted principal stress difference field with our experimentally observed flow birefringence principal stress difference contours [29, 30]. The concept of a “cost function” has been used in order to make a quantitative comparison.

The cost function quantifies the difference between an experiment (for example a birefringence pattern – see Fig. 4 and 7) and a numerical result (for example a distribution of principal stress difference (see Fig. 4). In order to do this it is first necessary to derive a line contour pattern (skeleton) from the birefringence and then to make a quantitative comparison between the line wise experimental and numerical patterns. The work described in this section is mainly from as yet unpublished work from Nouatin [30].

5.1 Forming a Skeleton Birefringence Pattern

In general, it is not possible to identify all flow birefringence principal stress difference contours for the whole flow. Difficulties can arise in the down stream channel near the walls and optical light contrast can vary over the field of view. We therefore have to select flow zones where the comparison between experiment and computation is possible as shown in (Fig. 8A). We divide this flow zone into several sub zones in which the contrast of the photography is uniform. In each of these sub zones we select a “critical grey level” and then, using a thresh-holding technique, derive a black and white pattern as shown in (Fig. 8B). Finally in this black and white pattern we choose the median line of each of the fringes to form a “skeleton” of the birefringence pattern as shown in Fig. 8C.

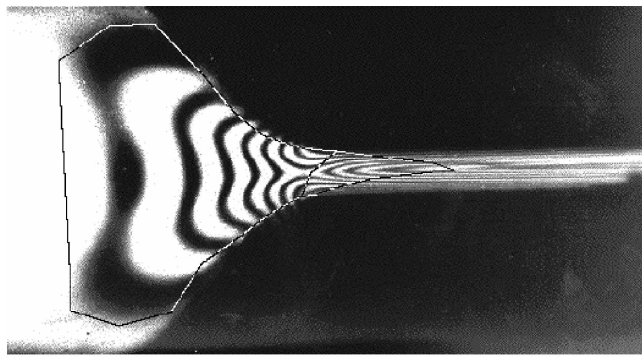
5.2 The Comparison Technique

Assuming the validity of the stress optical law, one can derive a stress pattern from the birefringence pattern (see for example [45, 46, 47].

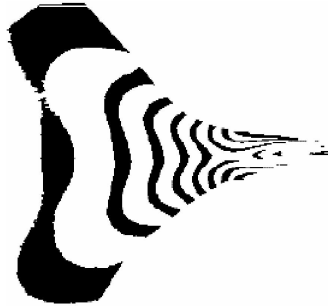
$$\Delta = C(\sigma_{11} - \sigma_{22}), \quad (1)$$

Δ is the birefringence, $(\sigma_{11} - \sigma_{22})$ is the principal stress difference and C is the stress optical coefficient which is assumed to be constant in the whole domain.

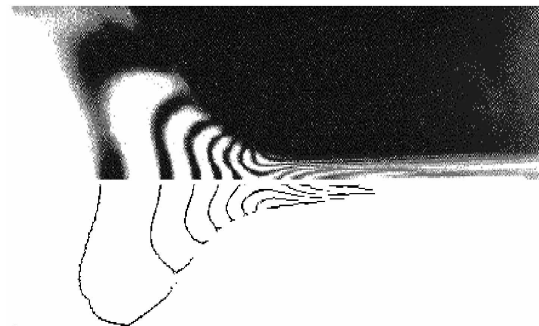
We now have two sets of line contour plots for the principal stress difference, one experimental and the other numerical



A)



B)



C)

Fig. 8. Successive steps of the birefringence pattern image analysis for the smooth convergent die

A: flow zones selection; B: image thresholding; C: image skeletonisation and comparison with the initial pattern, see [29] for further details

and these need to be quantitatively ranked against each other. This was done using a normalisation technique developed specifically for this task.

The line contours for both experiment and simulation were set as being black and between each adjacent contour line a grey level was set that was proportional to the distance from each line. In this way each coordinate point ij had a specified grey level. This procedure was carried out for both the numerical and the experimental contours.

A normalised cost function F was defined that compared the grey levels at different coordinate positions in the chosen sub zone. The experimental birefringence pixel resolution was

taken for the appropriate coordinate dimensions.

$$F = \sqrt{\sum_{i=1}^n \sum_{j=1}^m \frac{(G_{ij}^{sim} - G_{ij}^{exp})^2}{(G_{ij}^{exp})^2}}, \quad (2)$$

(i, j) are the pixels of the two normalised patterns, G_{ij}^{sim} is the grey level of the normalised simulation pattern. G_{ij}^{exp} is the grey level of the normalised experimental pattern.

In Fig. 9A an experimental birefringence pattern and a matching numerical simulation is superimposed on each other. The results are good, but not a perfect match and Fig. 9B indicates the difference between the two patterns: if Fig. 9B is totally white, the agreement is perfect, if Fig. 9B is totally black, the agreement is very bad.

By computing the cost function defined above it is possible to put a single number to the quality of the fit between experiment and simulation.

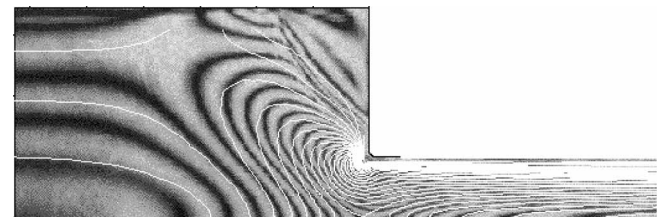
5.3 Using ART to Optimise Rheological Parameters; the Simplex Method

We are now in a position to use the cost function approach as a tool for optimising certain non linear parameters in a constitutive equation in order to obtain a best fit between the experimental and numerical global stress field. This is done by testing different constitutive parameters and obtaining a minimum to the cost function.

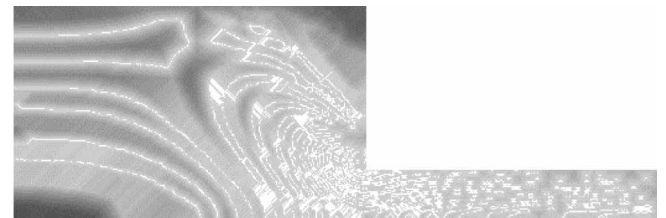
Simulation has been carried out using a multimode Phan Thien Tanner (PTT) constitutive equation of the form given below.

$$\sigma = -pI + 2\eta_s D(\vec{u}) + \tau, \quad \tau = \sum_i \tau_i,$$

$$\exp\left(\frac{\varepsilon\lambda_i}{\eta_v} \text{tr}(\tau_i)\right) \tau_i + \lambda_i \left[\left(1 - \frac{a}{2}\right) \tau_i^\nabla + \frac{a}{2} \tau_i^\nabla\right] = 2\eta_{vi} D(u), \quad (3)$$



A)



B)

Fig. 9. Superposition of the experimental birefringence pattern and the numerical computation (A), principal stress difference and (B) grey level difference between the two patterns, see [29] for further details

p is the pressure, \bar{u} the velocity field and $D(\bar{u})$ the rate of strain tensor. η_s is a “solvent viscosity”. λ_i and η_i are the relaxation times and the corresponding viscosities which were deduced from dynamic shear measurements. The symbols τ_i^∇ and τ_i^Δ denote the upper and lower convected derivatives of τ_i .

The non linear parameters in the constitutive equation that we wish to identify and optimise are coefficients a and ε .

The simplex method [48] was used in order to perform the minimisation of the cost function. The method needs only the evaluation of the cost function by direct simulation for different estimated parameters. After each step the set of parameters giving the highest value of the cost function is eliminated and replaced by a set giving lower values using the following specific operators: reflexion, expansion and contraction. The procedure is repeated until minimum value of the cost function is reached and these values of (a, ε) are then assumed to be the optimal.

5.4 The Application of ART

Results for a DSM polyethylene are given in this paper as one example of how the ART model can be used to identify the non linear parameters. The Multi mode (PTT) constitutive equation was chosen and the discrete spectrum of relaxation times and viscosities for this material are given in [29].

Three semi arbitrary initial values of the non linear parameters

(a, ε) (1. 2. 3. on Fig. 10) where chosen and the cost function evaluated for each of these simulations. The cost function lies between 22 and 23 %. Using these values and the simplex method for optimisation, further iterations were carried out and after convergence (point 9 in Fig. 10), the cost function has reduced to 1.2 % and the agreement with the experimental birefringence pattern is good, as shown in Fig. 4. It can therefore be seen from this one example that it is possible to optimise certain parameters within the constitutive equation in order to establish best fit values for the parameters. A further test, to carry out, is to use the optimised parameters established for one flow condition and for a particular geometry and establish whether these parameters give an equally low cost function for another set of flow conditions and or geometries. Initial results are encouraging.

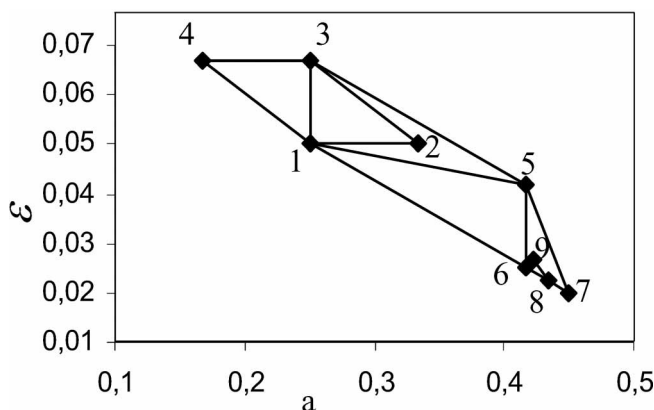


Fig. 10. Plot of the iteration for successive steps of the simplex method. ε and a are the non linear parameters in the PTT model and the data shows the progressive iteration of the ART module to a minimum cost function value

6 Conclusions and Future Perspectives

We have described experimental processing flows and matching numerical simulations for a number of situations and have also shown for one test case that it is now possible to quantitatively match laboratory experimental flow situations with numerical simulation and optimise certain rheological parameters in order to obtain the best fit between the experimental result and numerical simulation. This procedure can thereby avoid the use of restricted extensional rheological data and gives an alternative and possibly more accurate route to polymer process simulation.

The work raises a number of central issues in relation to the prediction of polymer processing. Firstly it seems clear that linear viscoelastic characterisation is adequately modelled by a multi mode approach providing an adequate number of relaxation modes are included. Currently all our numerical simulations of viscoelastic flows have started from this point. The choice of the appropriate constitutive equation that captures the correct form of non linear response is still an open debate. In addition the way in which non linear rheological data are obtained over a wide range of strains and strain rates is also still a very open experimental question.

In this paper, four non rheometric “prototype industrial flows” have been considered. In three cases experimental flow birefringence data has been obtained for different process conditions. Equally a number of different numerical solvers using different constitutive equations have been used to numerically simulate the different prototype industrial flows.

An ART model has been developed that enables the numerical simulation to be quantitatively ranked against the experimental observations and a simplex optimisation procedure has been used to optimise certain non linear parameters in order to obtain the best fit between experiment and simulation. The initial results presented here for one case study are encouraging in that the simplex method was found to rapidly converge to a result that gave very good matching.

The prototype industrial flows that have been considered in this paper represent complex flow situations that have strong similarities to many commercial processes, and consequently the results that we have obtained give confidence that the approach could be usefully used for commercial application.

There are still a number of uncertainties on the route to a full numerical simulation of viscoelastic processing flow. Much, but not all, of our work has been restricted to two dimensional flow and it is clear that in the future three dimensional solvers will be necessary if real processes are to be simulated. This raises serious issues in relation to computing time which can already be typically days for some of the simulations carried out. There continues to be a need to refine and understand the form of constitutive equation and this is an issue that is unlikely to be quickly resolved. Some of our work has also highlighted the need to consider fluid boundary conditions with great care. Finally, both compressibility and non isothermal effects need to be taken into account. It is however clear that the current position is now adequate for both scientists and polymer process engineers to use numerical simulation of viscoelastic process flow as a design tool.

References

- 1 Larson, R. G.: Constitutive equations for polymer melts and solutions, Butterworths, Boston (1988)
- 2 Dealy, J. M., Wissbrun, K. F.: Melt Rheology And Its Role In Plastics Processing: Theory And Applications. Chapman & Hall, New York (1995)
- 3 McLeish, T. C. B., Larson, R. G.: J. Rheol. p. 81 (1998)
- 4 Wagner, M. H., Schaeffer, J.: Rheo. Acta 33, p. 506 (1994)
- 5 Crochet, M. J., Walters, K.: Computational Rheology-A new Science Endeavour 2, p. 64 (1993)
- 6 Rajagopalan, D., Armstrong, R. C., Brown, R. A.: J. Non-Newtonian Fluid Mech. 36, p. 159 (1990)
- 7 Debbaut, B., Marchal, J. M., Crochet, M. J.: J. Non-Newtonian Fluid Mech. 29, p. 119 (1988)
- 8 Debae, F., Legat, V., Crochet, M. J.: J. Rheol. 38, p. 421 (1994)
- 9 Keunings, R., in: Computer Modeling for Polymer Processes, Tucker III, C. L. (Ed.), Carl Hanser München (1989)
- 10 Keunings, R.: A Survey of Computational Rheology. Proceeding of X111 Int. Cong. Rheology, Cambridge (2000)
- 11 Baaijens, F. P. T., Verbeeten, W. M. H., Peters, G. W. M.: Analysis of Viscoelastic Polymer Melt Flow. Proceeding of X111 Int. Cong. Rheology, Cambridge (2000)
- 12 Baaijens, F. P. T.: J. Non-Newtonian Fluid Mech. 79 p. 361 (1998)
- 13 Goublomme, A., Draily, B., Crochet, M. J.: J. Non-Newtonian Fluid Mech. 44, p. 171 (1992)
- 14 Kiriakidis, D. G., Park, H. J., Mitsoulis, E., Vergnes, B., Agassant, J. F.: J. Non-Newtonian Fluid Mech. 47, p. 339 (1993)
- 15 Hannachi, A., Mitsoulis, E.: Adv. Polym. Tech. 3, p. 217 (1993)
- 16 Ahmed, R., Liang, R. F., Mackley, M. R.: J. Non-Newtonian Fluid Mech. 59, p. 129 (1995)
- 17 Wagner, M. H., Laun, H. M.: Rheol. Acta 17, p. 138 (1978)
- 18 Beraudo, C., Fortin, A., Coupez, T., Demay, Y., Vergnes, B., Agassant, J. F.: J. Non-Newtonian Fluid Mech. 75, p. 1 (1998)
- 19 Langouche, F., Debbaut, B.: Rheol. Acta 1, p. 48 (1999)
- 20 Phan Thien, N., Tanner, R. I.: J. Non-Newtonian Fluid Mech. 2, p. 353 (1977)
- 21 Giesekus, H.: J. Non-Newtonian Fluid Mech. 11, p. 69 (1982)
- 22 Inkson, N. J., McLeish, T. C. B., Harlen, O. G., Groves, D. J.: J. Rheol. 43, p. 873 (1999)
- 23 Bishko, G. B., Harlen, O. G., McLeish, T. C. B., Nicholson, T. M.: J. Non-Newtonian Fluid Mech. 82, p. 255 (1999)
- 24 Verbeeten, W. M. H., Peters, G. W. M., Baaijens, F. P. T.: submitted to Journal of Rheology
- 25 Wagner, M. H., Rubio, P., Bastian, H.: submitted to Journal of Rheology
- 26 Wagner, M. H.: Korea-Australia Rheology Journal 11, p. 293 (1999)
- 27 Honnerkamp, J., Weese, J.: Rheol. Acta. 32, (1993)
- 28 Winter, H. H.: J. Non-Newtonian Fluid Mech. 68, p. 225 (1997)
- 29 Nouatin, O. H., Gravrus, L., Coupez, T., Vergnes, B., Agassant, J. F.: Inverse method for the identification of the rheology of molten polymers. Proceeding of X111 Int. Cong. Rheology, Cambridge (2000)
- 30 Nouatin, O. H.: Ph.D. Thesis Ecole des Mines de Paris Sophia Antipolis, France (2000)
- 31 Schoonen, J. F. M., Swartjes, F. H. M., Peters, G. W. M., Baaijens, F. P. T., Meijer, H. E. H.: J. Non-Newtonian Fluid Mech. 79, p. 529 (1998)
- 32 Peters, G. W. M., Schoonen, J. F. M., Baaijens, F. P. T., Meijer, H. E. H.: J. Non-Newtonian Fluid Mech. 82, p. 387 (1999)
- 33 Wagner, M. H., Bernnat, A., Schulze, V.: J. Rheol. 42, p. 917 (1998)
- 34 Bernnat, A., Wagner, M. H.: Int. Polym. Process. 3, p. 336 (1999)
- 35 Bernnat, A., Wagner, M. H., Carrot, C., Fulchiron, R.: Proceeding X111 Int. Cong. Rheology, Cambridge (2000)
- 36 Mackley, M. R., Spitteler, P. H. J.: Rheol. Acta. 35, p. 202 (1996)
- 37 Mackley, M. R., Marshall, R. T. J., Smeulders, J. B. A. F.: J. Rheol. 6, p. 1293 (1995)
- 38 Lee, K., Mackley, M. R.: Proceeding of X111 Int. Cong. Rheology, Cambridge (2000)
- 39 Crochet, M. J., Debbaut, B., Keunings, R., Marchal, J. M.: in Extrusion and Other Continuous Processes. O'Brien, K. T., (Ed.), Carl Hanser, München 1992
- 40 Polyflow User's manual, version 3.8.0, Fluent Inc. (2000)
- 41 Baaijens, F. P. T., Selen, S. H. A., Baaijens, H. P. W., Peters, G. W. M., Meijer, H. E. H.: J. Non-Newtonian Fluid Mech. 68, p. 173 (1998)
- 42 Goublomme, A., Crochet, M. J.: J. Non-Newtonian Fluid Mech. 47, p. 281 (1993)
- 43 Yao, M., McKinley, G. B. H., Debbaut, B.: J. Non-Newtonian Fluid Mech. 79, p. 469 (1998)
- 44 Debbaut, B., Dooley, J.: J. Rheol. 6, p. 1525 (1999)
- 45 Müller, R., Vergnes, B.: in Rheology for Polymer Processing. Piau, J. M., Agassant, J. F. (Eds.), Elsevier, New York
- 46 Janeschitz-Kriegl, H.: Polymer Melt Rheology and Flow Birefringence. Springer-Verlag, Berlin (1983)
- 47 Lodge, T. P., in Macosko, C. W.: Rheology, Principles, Measurements and Applications. (Ed.), VCH Publisher, New York, Weinheim (1994)
- 48 Nelder, J. A., Read, R.: The Computer Journal 7, p. 308 (1965)

Acknowledgements

We would like to thank the EU for the financial support of this project (BPRP-CT 9660278) and also thank the participating companies and universities for making this research programme possible. MRM would particularly like to thank CNRS and CEMEF for the opportunity to work at Sophia Antipolis, which greatly assisted the preparation of this paper.

Date received: September 12, 2001

Date accepted: January 16, 2002